Haploinsufficiency of the Mus81–Eme1 endonuclease activates the intra-S-phase and G_2/M checkpoints and promotes rereplication in human cells

Takashi Hiyama[1,3], Mari Katsura[1], Takashi Yoshihara[1], Mari Ishida[1], Aiko Kinomura[1], Tetsuji Tonda[2], Toshimasa Asahara[3] and Kiyoshi Miyagawa[1,4,*]

[1]Department of Human Genetics and [2]Department of Environmetrics and Biometrics, Research Institute for Radiation Biology and Medicine and [3]Department of Surgery, Graduate School of Biomedical Sciences, Hiroshima University, 1-2-3 Kasumi, Minami-ku, Hiroshima 734-8553, Japan and [4]Section of Radiation Biology, Graduate School of Medicine, The University of Tokyo, 7-3-1 Hongo, Bunkyo-ku, Tokyo 113-0033, Japan

ABSTRACT

The Mus81–Eme1 complex is a structure-specific endonuclease that preferentially cleaves nicked Holliday junctions, 3′-flap structures and aberrant replication fork structures. $Mus81^{-/-}$ mice have been shown to exhibit spontaneous chromosomal aberrations and, in one of two models, a predisposition to cancers. The molecular mechanisms underlying its role in chromosome integrity, however, are largely unknown. To clarify the role of Mus81 in human cells, we deleted the gene in the human colon cancer cell line HCT116 by gene targeting. Here we demonstrate that Mus81 confers resistance to DNA crosslinking agents and slight resistance to other DNA-damaging agents. Mus81 deficiency spontaneously promotes chromosome damage such as breaks and activates the intra-S-phase checkpoint through the ATM-Chk1/Chk2 pathways. Furthermore, Mus81 deficiency activates the G_2/M checkpoint through the ATM-Chk2 pathway and promotes DNA rereplication. Increased rereplication is reversed by the ectopic expression of Cdk1. Haploinsufficiency of Mus81 or Eme1 also causes similar phenotypes. These findings suggest that a complex network of the checkpoint pathways that respond to DNA double-strand breaks may participate in some of the phenotypes associated with Mus81 or Eme1 deficiency.

INTRODUCTION

Precise replication of the entire genome during the S phase of the cell cycle is essential for cell survival. The progression of replication forks can be stalled in response to exogenous and endogenous sources, including depletion of deoxyribonucleotide pools, inhibition of replication proteins and aberrant DNA structures. Stalled replication forks can degenerate into broken forks, leading to chromosomal rearrangements and deletions (1). To avoid such deleterious events, all eukaryotes have evolved cell cycle checkpoint machinery and DNA repair pathways (2). The homologous recombination repair pathway contributes to the accurate repair of DNA damage; however, to promote cell survival, homologous recombination also participates in chromosomal rearrangements when replication forks are stalled (3).

Mus81 was originally identified as a member of the XPF family of endonucleases that physically interacts with Rad54 in *Saccharomyces cerevisiae* and Cds1 (Chk2) in *Schizosaccharomyces pombe* (4,5). The gene confers resistance to agents that lead to replication fork stalling or collapse, including ultraviolet (UV) radiation, methylmethane sulfonate (MMS), hydroxyurea and camptothecin, suggesting a role for Mus81 in the rescue of stalled and collapsed replication forks (6). In contrast, Mus81-deficient murine cells are not hypersensitive to camptothecin (7). The functional binding partner of the protein is MMS4 in *S.cerevisiae* (8) and Eme1 in *S.pombe* (9) and mammals (10–13). The synthetic lethality of *mus81* (or *mms4*) *sgs1* (or *top3*) double mutants suggests a functional link between Mus81 and Sgs1 helicases in the late steps of recombination (4,8). *In vitro*, the Mus81–Eme1 complex preferentially cleaves 3′-flap structures, various aberrant replication fork structures, and nicked Holliday junctions, suggesting that the complex plays a role in stalled replication fork processing and DNA repair by homologous recombination (14–16).

Loss of Mus81, MMS4 or Eme1 results in a reduction in sporulation and spore viability in yeast (8,9,17). Poor spore viability in *mus81* or *eme1* mutants of *S.pombe* is suppressed

---

by eliminating Rec6 or Rec12, proteins required for the formation of double-strand breaks (DSBs), which initiates meiotic recombination. Expression of the bacterial Holliday junction resolvase RusA has been found to rescue the *mus81* meiotic defect (9). Thus, Mus81, MMS4 and Eme1 have been implicated in the processing of homologous recombination intermediates in yeast meiosis. The role of the Mus81–Eme1 complex in mitotic homologous recombination in mammals, however, remains uncertain (10,11,18). Remarkably, both *Mus81*$^{+/-}$ and *Mus81*$^{-/-}$ mice exhibit a profound predisposition to lymphomas and other cancers (18), although a subsequent study found no increased susceptibility to cancer in a different *Mus81*$^{-/-}$ model (7).

The role of Mus81 in genome integrity in response to replication stress has been proposed to be related to its physical association with Cds1 (Chk2) in fission yeast (19). Cds1-dependent phosphorylation of Mus81 prevents it from cleaving stalled replication forks that lead to replication fork breakage and chromosomal rearrangements by dissociating it from chromatin in cells exposed to hydroxyurea. Spontaneous and mitomycin C (MMC)-induced DNA damage such as breaks and triradial exchanges is increased in *Mus81*$^{+/-}$ and *Mus81*$^{-/-}$ mouse cells. In addition to these aberrations, the mutant cells have been shown to have an increased rate of aneuploidy (18).

Despite accumulating evidence that Mus81 plays a role in the processing of aberrant replication fork structures, the molecular mechanisms underlying its role in chromosome stability remain unclear. To clarify the role of Mus81–Eme1 in human cells, we deleted the genes in the human colon cancer cell line HCT116 by gene targeting. The advantages of using this cell line are that it allows efficient gene targeting in the presence of an intact p53 gene (20) and the cellular ploidy is stable. Here we show that Mus81 deficiency activates the intra-S-phase and G₂/M checkpoints and promotes DNA rereplication. This promotion of DNA rereplication was reversed by the forced expression of Cdk1. These findings provide new insight into the role of the Mus81–Eme1 complex in the control of human cell ploidy.

MATERIALS AND METHODS

Gene targeting at the Mus81 and Eme1 loci in HCT116

Targeting vectors were designed for in-frame insertion of promoterless drug resistance genes in exon 3 of *Mus81* or in exon 2 of *Eme1*. A 2.5 kb 5′-homology arm of *Mus81* was amplified by PCR from the isogenic DNA of HCT116 cells using primers 5′-GCCATGTCCAACGTCAGTA-3′ and 5′-ATCGATTCTCTCCAGATGGTGAGT-3′. A 1.7 kb 3′-homology arm of *Mus81* was amplified using primers 5′-ATCGATACTTGCGGAAGTCCA-3′ and 5′-AGGCAG-AGGGGACAACACAG-3′. A 2.6 kb 5′-homology arm of *Eme1* was amplified using primers 5′-TTCACAGCACTTGC-CAGTCT-3′ and 5′-ATCGATAATCCAGTGAGGGTGAT-GAC-3′. A 1.8 kb 3′-homology arm of *Eme1* was amplified using primers 5′-ATCGATTGTGAAGCCTCCTGTCCT-3′ and 5′-GGAACTGTCCTGTGTTACTG-3′. Both arms were cloned into pCR2.1 (Invitrogen) by the TA cloning method. The 3′-arms of *Mus81* and *Eme1* were excised by digestion with ClaI/SpeI and ClaI/XhoI, respectively, and subcloned

into the vectors containing the 5′-arms. Neomycin and blasticidin resistance cassettes were inserted into the ClaI site of the vector containing both arms. Gene targeting in HCT116 was performed as described previously (21).

Ectopic expression of the Mus81 and Eme1 cDNAs

The human *Mus81* cDNA was amplified by PCR from cDNA derived from normal human cells using primers 5′-TGAT-CTCAACGGTCCTGC-3′ and 5′-GGGCTGTTTCACGGC-ATAA-3′. The human *Eme1* cDNA was amplified using primers 5′-AGTTGAAAGAGTGGCGGGA-3′ and 5′-CTCA-TCCCTGAGGGCTAGAA-3′. The cDNAs were inserted into pCR2.1, and the sequences were confirmed. The expression vectors were designed to insert the genes under the control of the MSV enhancer and the MMTV promoter. Transfected cells were selected in the presence of 900 μg/ml Zeocin™ (Invitrogen).

Sensitivity to DNA-damaging agents

Sensitivity to MMC was measured as described previously (22). To measure sensitivity to hydroxyurea, we plated the cells at a density of 2×10^3 cells per 60 mm dish, treated them with the agent for 6 h, and washed them three times with phosphate-buffered saline (PBS). To measure the sensitivity to UV treatment, we plated the cells at the same density and irradiated them. After 7 days of culturing, colonies were counted. Sensitivity to other DNA-damaging agents was measured as described previously (21). When knockout or complemented cells showed slow growth compared to wild-type cells, colonies were further cultured for 2 to 3 days and counted.

Focus formation of Rad51 and Rad54

Radiation-induced focus formation of Rad51 and Rad54 was performed as described previously (21). MMC-induced focus formation was examined by treatment with 0.8 μg/ml MMC for 1 h.

Cell cycle analysis

Cell synchronization by double-thymidine block was performed as described previously (23). Flow cytometry was performed with a FACSCalibur (Becton Dickinson) using the CellQuest software package.

Kinase assay

Immunoprecipitation was performed in the presence of phosphatase inhibitors (5 μM cantharidin, 5 nM microcystin LR and 25 μM bromotetramisole oxalate) essentially as described (22). Immunoprecipitates were washed three times in lysis buffer and three times in 25 mM HEPES (pH 7.4). The kinase reaction was performed at 30°C for 20 min in a total of 40 μl of reaction buffer [25 mM HEPES (pH 7.4), 15 mM MgCl₂, 80 mM EGTA, 1 mM DTT, 0.1 mM ATP and 3 μCi [γ-³²P]ATP]. Histone H1 (10 μg) was used as a substrate for the cyclin E, cyclin A and cyclin B kinase assays. Glutathione *S*-transferase (GST)-Cdc25C (200–256) was used as a substrate for the Chk2 kinase assay and was prepared as follows. The Cdc25C (200–256) fragment was amplified by PCR from cDNA derived from normal human cells using primers 5′-GAAAGATCAAGAAGCAAAGGTGAGC-3′ and 5′-TA-AGCCCTTCCTGAGCTT-3′ and inserted into pGEX-5X-1

(Amersham Pharmacia). The plasmid was then used to transform *Escherichia coli* BL21, and expression of the fusion protein was induced by adjusting the culture to 1 mM Isopropyl-β-D-thiogalactopyranoside (IPTG). The fusion protein was purified using a glutathione–Sepharose 4B column (Amersham Pharmacia). The kinase reaction products were boiled in sample buffer and analyzed by SDS–PAGE.

Antibodies

Antibodies to Mus81 (N-20), cyclin A (C-19), cyclin E (C-19), cyclin B1 (GNS1), Cdc2 (Cdk1) (17), Cdk2 (D-12), Chk2 (A-12), Chk1 (G-4), ATR (N-19) and actin (C-2) were from Santa Cruz Biotechnology. Antibodies to phospho-Chk2 (Thr-68), phospho-Chk1 (Ser-317) and p21 (DCS60) were from Cell Signaling Technology. The antibody to ATM (NB100–104) was from Novus Biologicals.

Immunofluorescence

Cells were grown overnight on coverslips and fixed for 10 min in 4% paraformaldehyde. Cells were blocked with 10% horse serum and incubated with primary antibodies at room temperature for 1 h and with secondary antibodies for 30 min. Finally, cells were counterstained with 4′,6′-diamidino-2-phenylindole (DAPI) and mounted.

siRNA transfection

Eight hours prior to transfection, cells for the assay of ATM and ATR expression were seeded in a 100 mm dish at 1×10^6 cells/dish. Cells for immunofluorescence were seeded on coverslips at 1×10^5 cells/coverslip. The siRNA sequences for ATM used in the study were 5′-CAUCUAGAUCGGC-AUUCAGtt-3′ and 5′-UGGUGCUAUUUAACGGAGCUtt-3′. The siRNA sequence for ATR was 5′-AACCUCCGUGAU-GUUGCUUGAtt-3′. These siRNAs were synthesized by Sigma Genosys. A siCONTROL nontargeting siRNA from Dharmacon was used as a negative control. Transfection was performed using Lipofectamine 2000 transfection reagent (Invitrogen) according to the manufacturer's instructions. For western blot analysis, the Lipofectamine–siRNA complex was not removed during incubation. Cells were harvested at 48 h post-transfection. For immunofluorescence after double-thymidine block, the transfection mixture was removed after the first thymidine block.

Ectopic expression of Cdk1

The human *Cdk1* cDNA was amplified by PCR from cDNA derived from normal human cells using primers 5′-GCTCTT-GGAAATTGAGCGGA-3′ and 5′-AGAAGACGAAGTACA-GCTGAAGT-3′. The cDNAs were inserted into pCR2.1, and the sequences were confirmed. The *Cdk1* expression vector was designed to insert the gene under the control of the MSV enhancer and the MMTV promoter. Cdk1-overexpressing cells were selected in the presence of 900 μg/ml Zeocin™ (Invitrogen).

RESULTS

Generation of Mus81-deficient HCT116 cells

To investigate Mus81 function in human cells, we inactivated its gene in HCT116 cells by gene targeting. Targeting vectors were designed such that exon 3 was disrupted by promoterless antibiotic-resistance genes (Figure 1A). We obtained two independent $Mus81^{+/-}$ clones from 744 neomycin-resistant colonies and two $Mus81^{-/-}$ clones from 2380 neomycin- and blasticidin-resistant colonies derived from a single $Mus81^{+/-}$ clone (#653). Southern blot analysis using both 5′- and 3′-probes confirmed that both wild-type alleles had been correctly inactivated by gene targeting in the $Mus81^{-/-}$ cells (Figure 1B). Northern blot analysis revealed no expression of the gene in these clones (Figure 1C). Because no additional bands were detected using the full-length *Mus81* cDNA as a probe, it is unlikely that aberrant transcripts were generated by the disruption of exon 3. The correct targeting events were confirmed by western blot analysis (Figure 1D). Levels of expression comparable to or much higher than that of endogenous expression were achieved in these mutants by the introduction of the human *Mus81* cDNA.

Generation of Eme1-deficient HCT116 cells

To compare the role of Mus81 in human cells with that of Eme1, exon 2 of *Eme1* was disrupted by a neomycin resistance gene (Figure 1E). We obtained two independent $Eme1^{+/-}$ cells from 5250 neomycin-resistant colonies. $Eme1^{-/-}$ cells were not successfully generated because $Eme1^{+/-}$ cells grow slowly; however, $Eme1^{+/-}$ cells were sufficient for the purpose of comparing the roles of these proteins. Southern and northern blot analyses confirmed the disruption of one allele of the gene (Figure 1F and G). A level of expression comparable to that of endogenous expression was achieved by the expression of human *Eme1* cDNA in $Eme1^{+/-}$ cells.

Roles of the Mus81–Eme1 complex in the sensitivity to DNA damage

We next examined the sensitivity of Mus81 or Eme1 mutant cells to DNA damage by measuring their ability to form colonies following exposure to DNA-damaging agents. Because knockout cells and some complemented cells grew slowly, we took the growth rate into account in the counting of colonies (see Materials and Methods). Modest sensitivity to MMC was observed in $Mus81^{+/-}$ cells (1.5-fold) and $Mus81^{-/-}$ cells (4-fold) (Figure 2A). We noted a similar mild sensitivity to cisplatin in $Mus81^{-/-}$ cells. Mus81 deficiency resulted in a slight sensitivity to UV radiation, MMS, hydroxyurea and ionizing radiation (Figure 2B–G). The expression of *Mus81* cDNA in $Mus81^{-/-}$ cells restored the sensitivities to DNA-damaging agents to the wild-type levels. A slight increase in sensitivity to cisplatin, UV radiation and hydroxyurea was observed in $Mus81^{+/-}$ cells. A similar sensitivity to MMC and hydroxyurea was found in $Eme1^{+/-}$ cells. The expression of Eme1 only partially complemented the sensitivity to MMC. This is probably explained by the level of Eme1 expression in complemented cells: even if levels comparable to the endogenous levels are achieved by constitutive expression, they may not be sufficient for full complementation in response to DNA damage. Furthermore, the level of Mus81 expression is strictly dependent on the cell cycle (24), and the peak of Mus81 expression occurs in the S and G_2 phases. Like Mus81 expression, Eme1 expression may vary according to the stage of the cell cycle. These results indicate that Mus81 and Eme1 contribute to the resistance
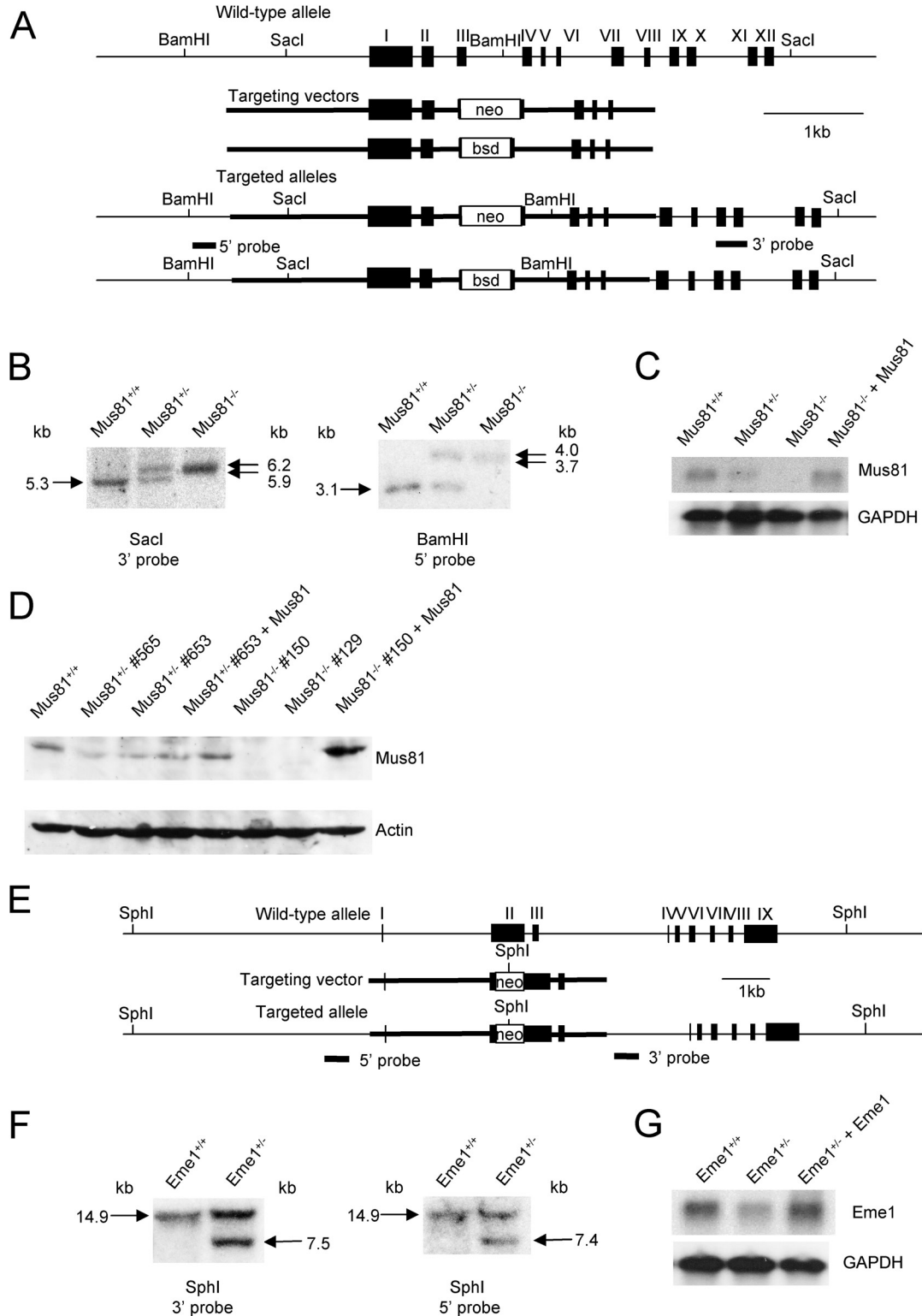
Figure 1. Generation of HCT116 cell lines deficient in Mus81 or Eme1 by gene targeting. (**A**) Schematic representation of the *Mus81* locus, the targeting vectors, and the targeted alleles. Relevant restriction sites and the position of the probes used for Southern blot analysis are shown. (**B**) Southern blot analysis confirming targeted integration at the *Mus81* locus. DNAs were digested with SacI or BamHI and hybridized with the probes depicted in (A). (**C**) Northern blot analysis confirming the expression levels of *Mus81*. Poly(A)$^+$ RNAs were isolated and hybridized with the full-length *Mus81* cDNA. Northern blotting for glyceraldehyde 3-phosphate dehydrogenase (GAPDH) was performed to confirm equal loading. (**D**) Western blot analysis confirming the protein expression levels of Mus81. Western blotting for actin was also carried out to confirm equal loading. (**E**) Schematic representation of the *Eme1* locus, the targeting vector and the targeted allele. Relevant restriction sites and the position of the probes used for Southern blot analysis are shown. (**F**) Southern blot analysis confirming targeted integration at the *Eme1* locus. DNAs were digested with SphI and hybridized with the probes depicted in (E). (**G**) Northern blot analysis confirming the expression levels of *Eme1*. Poly(A)$^+$ RNAs were isolated and hybridized with the full-length *Eme1* cDNA.
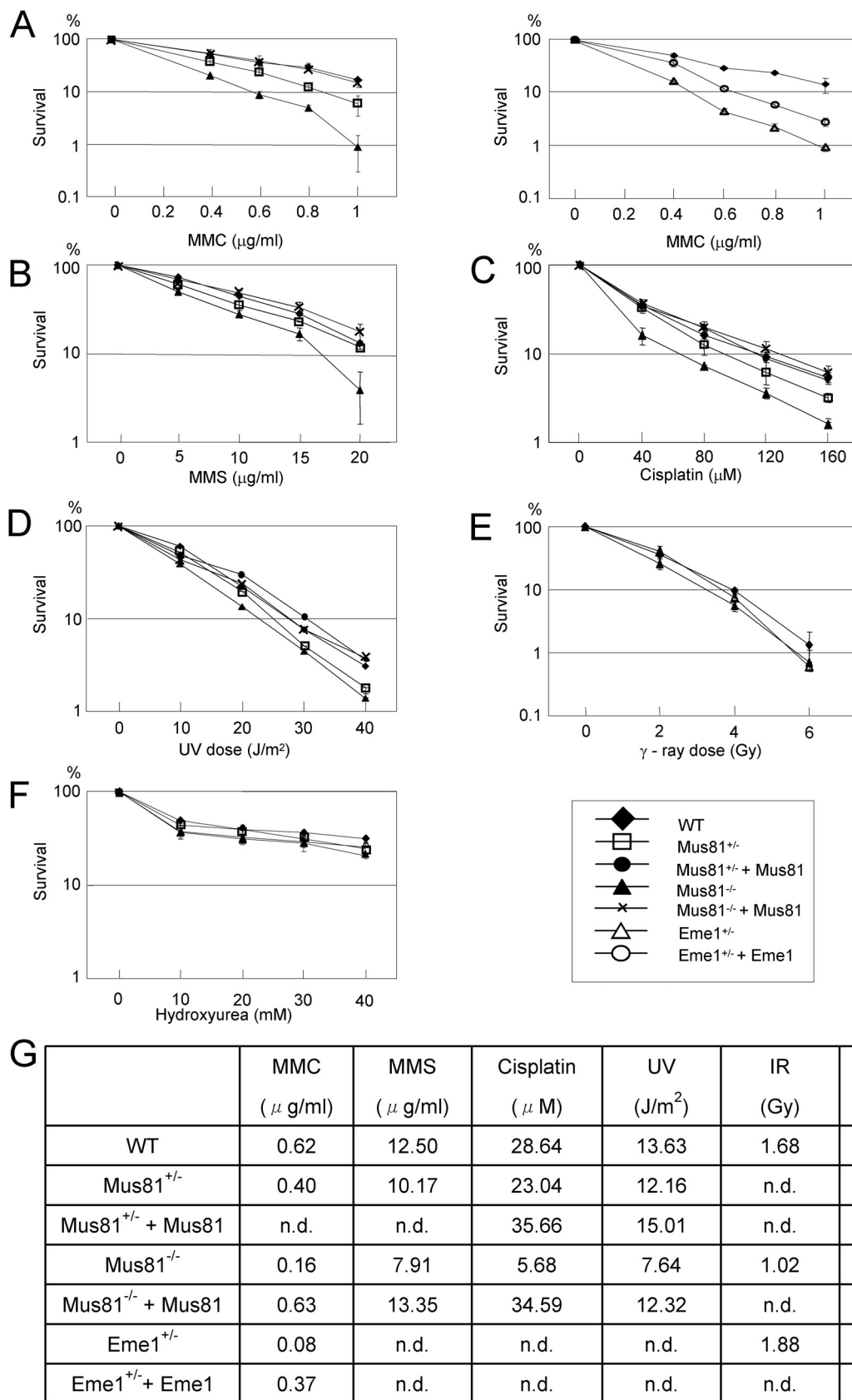
Figure 2. Sensitivity to DNA-damaging agents. (**A–F**) Sensitivities to MMC, MMS, cisplatin, UV radiation, ionizing radiation and hydroxyurea. Values represent the means ± the standard error of the mean for three independent experiments. *Mus81*^{+/−} (#653), *Mus81*^{−/−} (#150) and *Eme1*^{+/−} (#376) cells were used. (**G**) D37 values of sensitivity to DNA-damaging agents. Graph Pad Prism4 software was used to calculate the values.
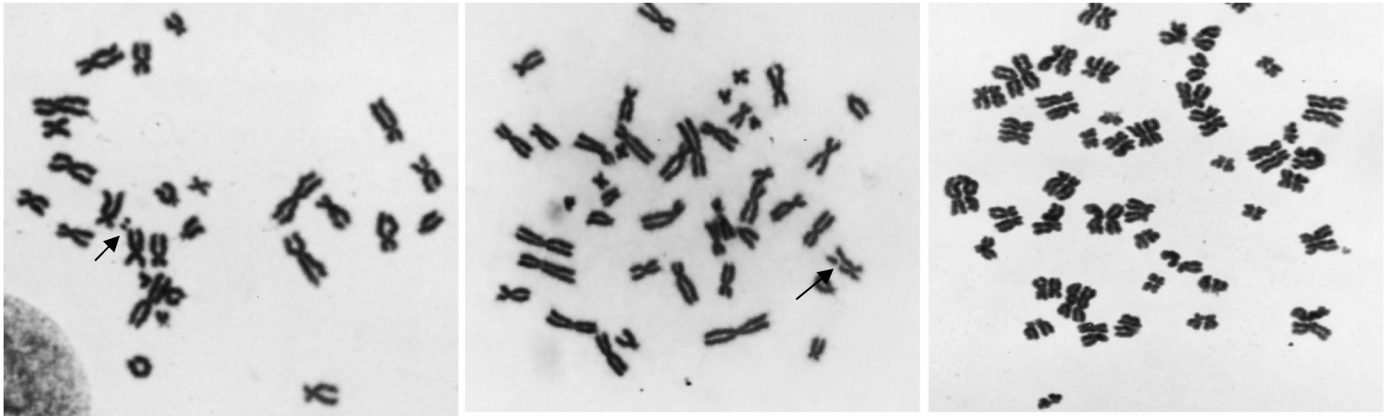
Figure 3. Chromosomal aberrations in $Mus81^{-/-}$ (#150) cells. The arrow in the left panel indicates a chromosome break. The arrow in the middle panel indicates a chromatid gap. Rereplication is shown in the right panel. In the left and middle panels, only a part of metaphase chromosome image is shown.

Table 1. Chromosomal aberrations

Cell line[a]	Chromatid-type[b] (%)	Chromosome-type[b] (%)	Abnormal cells[b] (excluding tetraploidy) (%)	Tetraploidy[c]
$Mus81^{+/+}$	2.5 ± 0.5	2.4 ± 1.1	4.5 ± 1.0	0.67% (23/3413)
$Mus81^{+/-}$	4.9 ± 1.2	6.2 ± 1.1	10.4 ± 1.1	1.88% (39/2077)
$Mus81^{+/-}$ + Mus81	3.2 ± 1.6	4.5 ± 1.5	6.7 ± 0.8	0.58% (6/1041)
$Mus81^{-/-}$	7.0 ± 1.3	10.0 ± 2.0	14.5 ± 0.5	2.46% (37/1503)
$Mus81^{-/-}$ + Mus81	2.4 ± 0.6	3.5 ± 1.5	5.7 ± 2.1	0.88% (27/3059)
$Mus81^{-/-}$ + Cdk1(#1)	6.2 ± 3.0	9.4 ± 4.1	12.9 ± 1.9	0.50% (10/2000)
$Mus81^{-/-}$ + Cdk1(#7)	4.0 ± 0.9	10.0 ± 0.5	11.2 ± 0.3	0.54% (6/1105)
$Mus81^{+/+}$ + Cdk1	2.5 ± 0.5	5.7 ± 1.6	6.9 ± 0.3	0.67% (2/300)
$Eme1^{+/-}$	6.4 ± 1.6	6.5 ± 1.3	10.7 ± 0.3	2.16% (63/2919)
$Eme1^{+/-}$ + Eme1	3.5 ± 0.9	5.2 ± 1.2	7.4 ± 1.3	1.20% (15/1248)

[a]$Mus81^{+/-}$ (#653), $Mus81^{-/-}$ (#150) and $Eme1^{+/-}$ (#376) cells were used.
[b]A total of 200 cells were scored for each line. Results represent the means ± SD of three independent experiments.
[c]The frequency of tetraploidy is shown as a percentage of tetraploid cells to the total number of metaphase cells analyzed; absolute numbers are given in parentheses.

of human cells to DNA-damaging agents such as DNA crosslinking agents.

Rad51 plays a central role in the early stages of homologous recombination and forms nuclear foci in a DNA damage-dependent manner (25). Impaired Rad51 focus formation has been reported in chicken and mammalian cells with defective homologous recombination (22,26,27). Rad54 plays a role in homologous recombination by dissociating Rad51 from nucleoprotein filaments formed on double-stranded DNA (28), and it forms nuclear foci that colocalize with foci of Rad51 (29). To investigate the role of Mus81 in the Rad51-dependent recombination pathway, we examined damage-dependent focus formation of Rad51 and Rad54 by treating cells with 0.8 µg/ml MMC or 8 Gy of ionizing radiation. We found no difference in focus formation between wild-type and $Mus81^{-/-}$ cells (data not shown), suggesting that Mus81 is not required for focus formation by these proteins.

Mus81–Eme1 is required for chromosome stability

A defect in homologous recombination repair leads to chromosome instability (30). We examined chromosomal aberrations in the presence of colcemid using metaphase spreads. The frequency of abnormal cells harboring chromatid- and chromosome-type aberrations such as gaps and breaks (Figure 3) was 4.5% in wild-type cells, whereas it increased to 10.4% in $Mus81^{+/-}$ cells and 14.5% in $Mus81^{-/-}$ cells (Table 1). Expression of the $Mus81$ cDNA partially complemented these phenotypes (6.7 and 5.7%, respectively). The number of cells showing abnormalities was also increased in $Eme1^{+/-}$ cells (10.7%), and it was reduced by the expression of the $Eme1$ cDNA (7.4%).

In addition to these aberrations, the numbers of tetraploid cells resulting from DNA rereplication (Figure 3) were significantly increased in the mutant cells (Table 1). The frequency of tetraploidy in wild-type cells was 0.67%, whereas it increased to 1.88% ($Mus81^{+/-}$) and 2.46% ($Mus81^{-/-}$) in the mutants. Differences in frequency were statistically significant between wild-type and $Mus81^{+/-}$ cells ($P < 1.0 \times 10^{-4}$) and $Mus81^{-/-}$ cells ($P < 1.0 \times 10^{-6}$). The differences were statistically evaluated using multiple logistic regression analysis taking Poisson errors into account. The expression of the $Mus81$ cDNA in the mutants reduced the number of tetraploid cells to a level that was comparable to wild-type cells. The frequency of tetraploid cells was also increased to 2.16% in $Eme1^{+/-}$ cells ($P < 1.0 \times 10^{-5}$), and this value was reduced to 1.20% by the expression of the $Eme1$ cDNA. Increases in DNA content resulting from DNA rereplication were not detected by FACS analysis, as only a small proportion of cells underwent rereplication.
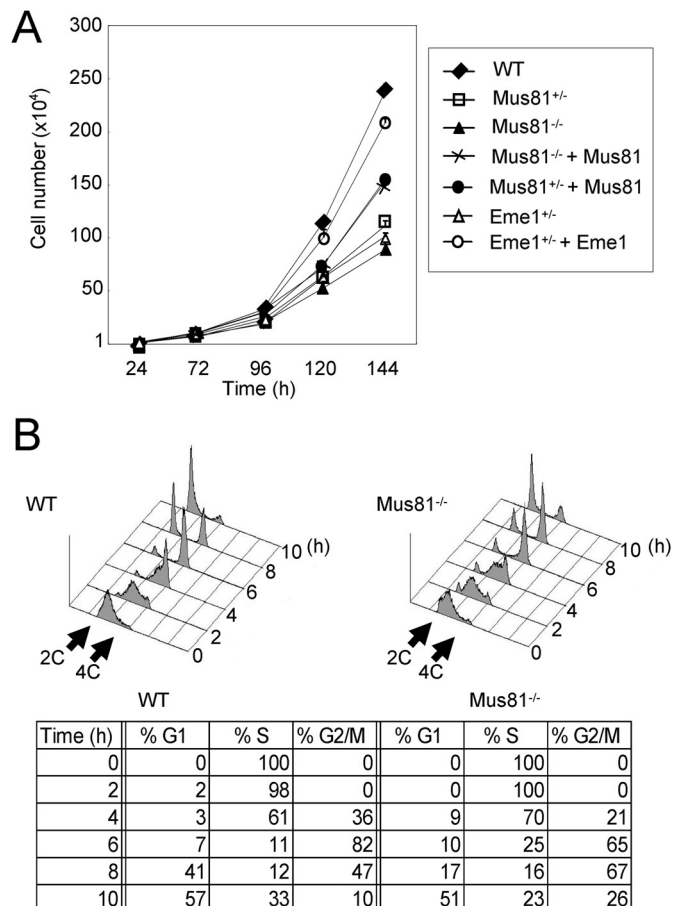
Figure 4. Effects of Mus81 or Eme1 deficiency on cell cycle progression. $Mus81^{+/-}$ (#653), $Mus81^{-/-}$ (#150) and $Eme1^{+/-}$ (#376) were examined. (**A**) Growth curves. The results show the means ± the standard error of the mean for three independent experiments. (**B**) Cell cycle distribution. The cells were synchronized in G_1/S by double-thymidine block and released. Samples were taken at the indicated time points and subjected to FACS analysis.

Time (h)	% G1	% S	% G2/M	% G1	% S	% G2/M
0	0	100	0	0	100	0
2	2	98	0	0	100	0
4	3	61	36	9	70	21
6	7	11	82	10	25	65
8	41	12	47	17	16	67
10	57	33	10	51	23	26

Mus81 or Eme1 deficiency affects cell cycle progression

The growth rates of $Mus81^{+/-}$, $Mus81^{-/-}$ and $Eme1^{+/-}$ cells were significantly lower than that of wild-type cells (Figure 4A). The doubling time of wild-type cells was 17 h, whereas the times for $Mus81^{+/-}$, $Mus81^{-/-}$ and $Eme1^{+/-}$ cells were 21, 22 and 21.5 h, respectively. Expression of the *Mus81* or *Eme1* cDNA partially complemented this phenotype. To examine the profiles of cell cycle progression, we performed FACS analysis using cells synchronized by double-thymidine block. We observed a small difference in the kinetics of accumulation of cells in the S and G_2/M phases between wild-type and $Mus81^{-/-}$ cells (Figure 4B). There was a peak in G_2/M phase accumulation 6 h after release in wild-type cells, whereas G_2/M phase accumulation was found 6 and 8 h after release in $Mus81^{-/-}$ cells.

Mus81 or Eme1 deficiency activates the intra-S-phase checkpoint

Cell cycle progression through S phase is regulated by cyclin E/Cdk2 and cyclin A/Cdk2. We therefore investigated the effects of Mus81 deficiency on the S phase progression by performing cyclin E and cyclin A kinase assays using lysates from cells synchronized in the G_1/S phase (Figure 5A). The cyclin E and cyclin A kinase activities were apparently lower in $Mus81^{-/-}$ cells than in wild-type cells at 0 and 0–8 h after release, respectively. Quantitative analysis revealed that $Mus81^{-/-}$ cells had a 40% reduction in cyclin E kinase activity at 0 h and a 50% reduction in cyclin A kinase activity at 4 h compared to wild-type cells. The levels of cyclin E and cyclin A in $Mus81^{-/-}$ cells were almost the same as in wild-type cells at this stage of the cell cycle, indicating that S phase checkpoint activation was responsible for the reductions in cyclin kinase activities.

Because the mutant cells showed a spontaneous delay of cell cycle progression during the S phase, we first investigated the effect of Mus81 deficiency on the ATR-Chk1 pathway, which regulates the basal turnover of Cdc25A (31). Western blot analysis using an anti-phospho-Chk1 antibody (Ser-317) revealed that levels of phospho-Chk1 were high in the early S phase and that the levels in $Mus81^{-/-}$ cells were the same as in wild-type cells (Figure 5B). This finding is consistent with the proposed role of Chk1 activation in the maintenance of the physiological turnover of Cdc25A.

However, the involvement of Chk1 in a DNA damage-dependent checkpoint cannot be evaluated by this method because the basal levels of phospho-Chk1 were high during the S phase. We therefore examined the damage-dependent Chk1 activation at the single-cell level by immunofluorescence using the same antibody (Figure 5C). Clear staining in the nucleus indicating the damage-dependent phosphorylation of Chk1 on Ser-317 was observed in a small proportion of cells. This staining pattern was found in $0.3 \pm 0.1\%$ (mean ± SD) of wild-type cells and in $1.9 \pm 0.1\%$ of $Mus81^{-/-}$ cells ($n = 500$). The frequencies of the staining ranged from $0.9 \pm 0.1\%$ to $1.5 \pm 0.2\%$ in $Mus81^{+/-}$ and $Eme1^{+/-}$ cells.

To investigate whether ATM or ATR regulates Chk1 activation by phosphorylation in the S phase, ATM and ATR were knocked down by siRNA (Figure 5D). Silencing of ATM reduced the frequency to $0.5 \pm 0.3\%$ in $Mus81^{-/-}$ cells, whereas silencing of ATR or transfection of control siRNA did not affect the frequency, indicating that the ATM-Chk1 pathway was activated in the S phase in $Mus81^{-/-}$ cells (Figure 5C). This pathway has been shown to be activated in response to DSBs induced by ionizing radiation (32).

The intra-S-phase checkpoint in response to DSBs was first shown to be mediated by the ATM-Chk2-Cdc25A-Cdk2 pathway (33). Next, we investigated Chk2 activation in the S phase by immunofluorescence using an anti-phospho-Chk2 (Thr-68) antibody (Figure 5E). Phosphorylation of Chk2 on Thr-68 is required for the initiation of Chk2 activity. Clear staining of phospho-Chk2 in the nucleus was not observed in wild-type cells, but it was observed in $2.3 \pm 0.3\%$ of $Mus81^{-/-}$ cells ($n = 500$). The frequency of the staining ranged from $1.0 \pm 0.2\%$ to $1.6 \pm 0.2\%$ in $Mus81^{+/-}$ and $Eme1^{+/-}$ cells, respectively. Silencing of ATM reduced the frequency to $0.7 \pm 0.5\%$, whereas silencing of ATR or transfection of control siRNA did not affect the frequency, indicating that ATM acted as an upstream kinase for Chk2 activation. Thus, both the ATM-Chk1 and ATM-Chk2 checkpoint pathways were activated during the S phase in the Mus81 and Eme1 mutant cells.
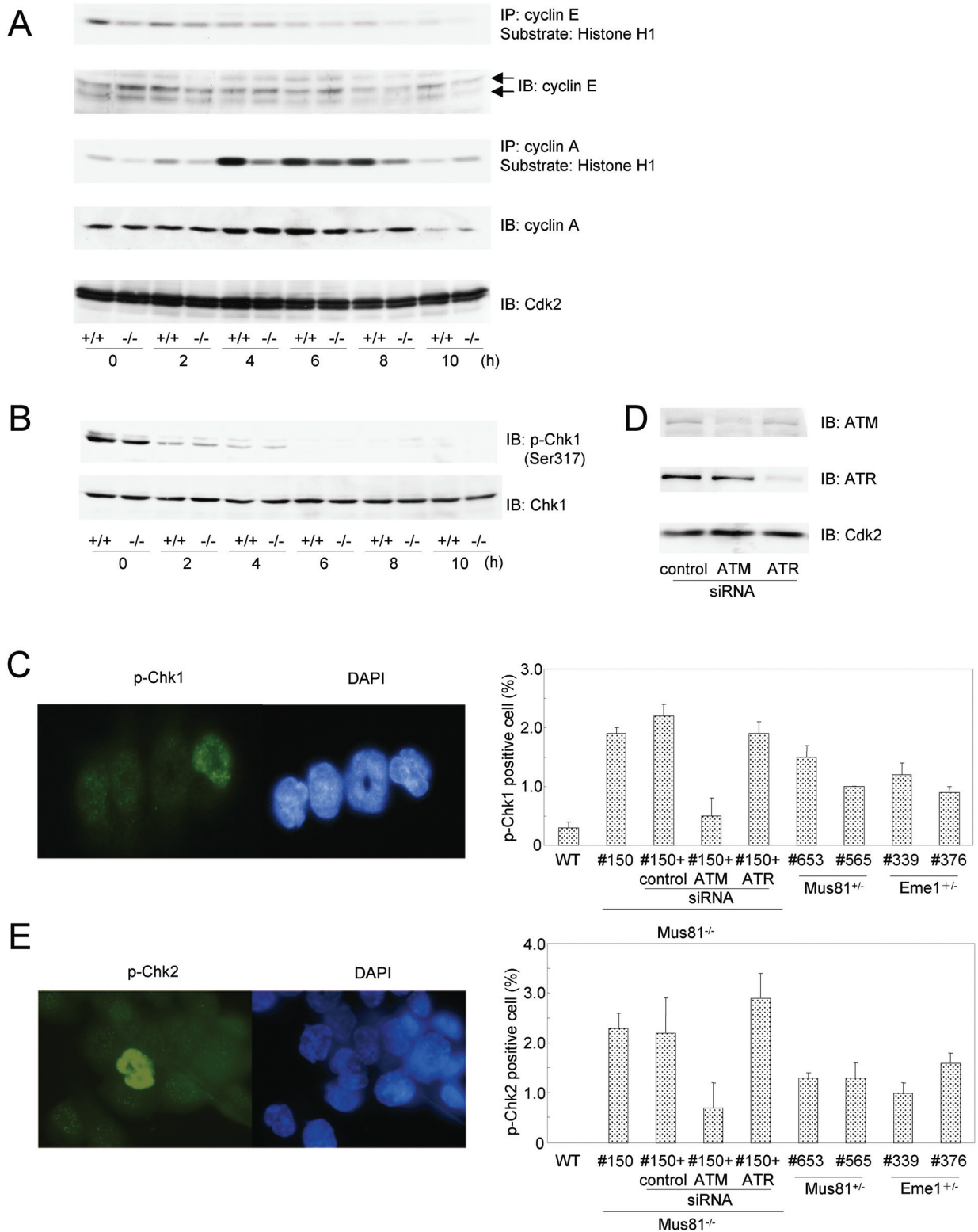
Figure 5. Activation of the intra-S-phase checkpoint. (**A**) Cyclin E and cyclin A kinase activities with histone H1 as the substrate. Wild-type and *Mus81*$^{-/-}$ (#150) cells were synchronized in G$_1$/S by double-thymidine block and released. (**B**) Western blot analysis of synchronized wild-type and *Mus81*$^{-/-}$ (#150) cell extracts using anti-phospho-Chk1 (Ser-317). The experiments in (A) and (B) were performed three times, and representative results are shown. (**C**) Immunofluorescence of *Mus81*$^{-/-}$ cells synchronized in S phase using anti-phospho-Chk1 (Ser-317). The frequencies of positive staining for phospho-Chk1 are shown in the right panel. (**D**) Western blot analysis of unsynchronized *Mus81*$^{-/-}$ (#150) cells transfected with siRNAs. The experiment was performed three times. (**E**) Immunofluorescence of *Mus81*$^{-/-}$ cells synchronized in S phase using anti-phospho-Chk2 (Thr-68). The frequencies of the positive staining of phospho-Chk2 are shown in the right panel. In (C) and (E), cells were fixed 2 h after release, and a total of 500 cells were examined for each cell line. The results represent the means ± standard deviation of three independent experiments. IB, immunoblot; IP, immunoprecipitation; p-Chk, phospho-Chk; WT, wild-type.

Mus81 or Eme1 deficiency activates the G$_2$/M checkpoint

Because FACS profiles revealed a difference in the accumulation of cells in G$_2$/M, we investigated the effects of Mus81 deficiency on the G$_2$/M delay by running a cyclin B kinase assay using cells synchronized in the G$_1$/S phase (Figure 6A). Cyclin B kinase activity was increased 6 h after release in wild-type cells, whereas an increase in the kinase activity was not obvious at 6 h but was clear at 8 h after release in the mutant. Repeated experiments demonstrated that such a difference between the wild-type and mutant cells could be observed either 6 or 8 h after release, consistent with the results from the FACS analysis. There were no apparent differences in cyclin B and Cdk1 levels between wild-type and *Mus81*$^{-/-}$ cells, excluding the possibility that reduced cyclin B kinase activity was due to repression of these proteins. In addition, we noticed that the level of cyclin B expression was high even in the G$_1$ phase at 10 h in the HCT116 cell line. This aberrant expression of cyclin B has been observed in some human cancer cells, suggesting that it may be associated with abnormal proliferation of cancer cells (34). The high level of cyclin B may account for the sustained cyclin B kinase activity during the early G$_1$ phase in wild-type cells.

Activation of Cdk1 by association with cyclin B is essential for the initiation of the M phase. The delay of cyclin B activity in *Mus81*$^{-/-}$ cells may simply indicate that the cell cycle progression was delayed by the preceding S phase delay. Alternatively, G$_2$/M checkpoint activation may be involved in the delay of cyclin B activity. Chk1 and Chk2 play a role in the G$_2$/M checkpoint as effector kinases (35). To investigate whether the G$_2$/M checkpoint was activated in the mutants, we therefore examined Chk1 and Chk2 kinase activities using a recombinant GST-Cdc25C (200–256) fusion protein as a substrate. These kinases preferentially phosphorylate Cdc25C on Ser-216 (36). We examined the difference in Chk2 kinase activity in synchronized cells. Chk2 kinase activity was significantly increased in the Mus81 mutant 6 h after release, whereas an increase was not evident in wild-type cells (Figure 6B). There were no differences in the levels of Chk2. A more than 3-fold increase in Chk2 activity was also observed in two *Mus81*$^{+/-}$ cell lines as well as in two *Eme1*$^{+/-}$ cell lines, excluding the possibility that activation of Chk2 was due to a clonal variation (Figure 6C). Expression of *Mus81* or *Eme1* cDNA reduced this increase in Chk2 activity in the mutant cells (Figure 6C). Chk2 kinase phosphorylation of Cdc25C was not clearly observed before 6 h, indicating that the increase in this activity at 6 h reflected the G$_2$/M checkpoint activation rather than a delay of the cell cycle progression. The S phase checkpoint was activated in *Mus81*$^{-/-}$ cells from 0 to 4 h after release.

The increase in Chk2 kinase activity was abolished in the presence of 0.5 mM caffeine (Figure 6C). Treatment with 0.5 mM caffeine for 1 h has little effect on DNA synthesis (37), excluding the possibility that the elimination of Chk2 activity by caffeine was due to the delay in cell cycle progression. Because caffeine inhibits ATM and ATR kinase activities (38–40), they are likely required for this increase in Chk2 kinase activity. For this reason, we further investigated the effect of siRNA silencing of ATM and ATR on Chk2 activity (Figures 5D and 6D). Chk2 activity was reduced by silencing

of ATM but not by silencing of ATR, indicating that the activation of ATM in response to DNA damage is responsible for the increase in Chk2 activity in *Mus81*$^{-/-}$ cells. In contrast, there was no clear difference in the phosphorylation of GST-Cdc25C (200–256) by Chk1 in wild-type and *Mus81*$^{-/-}$ cells (Figure 6E). There was also no difference in p21 expression in wild-type and *Mus81*$^{-/-}$ cells (Figure 6F).

It is assumed that the p21-dependent G$_2$/M checkpoint leads to sustained cell cycle arrest, whereas the Cdc25-dependent checkpoint leads to transient delay (41). Consistent with this idea, many delayed cells eventually proceeded into the M and G$_1$ phases. These results show that, in addition to the intra-S-phase checkpoint, the G$_2$/M checkpoint was activated in the Mus81 mutant cells via the ATM-Chk2 pathway.
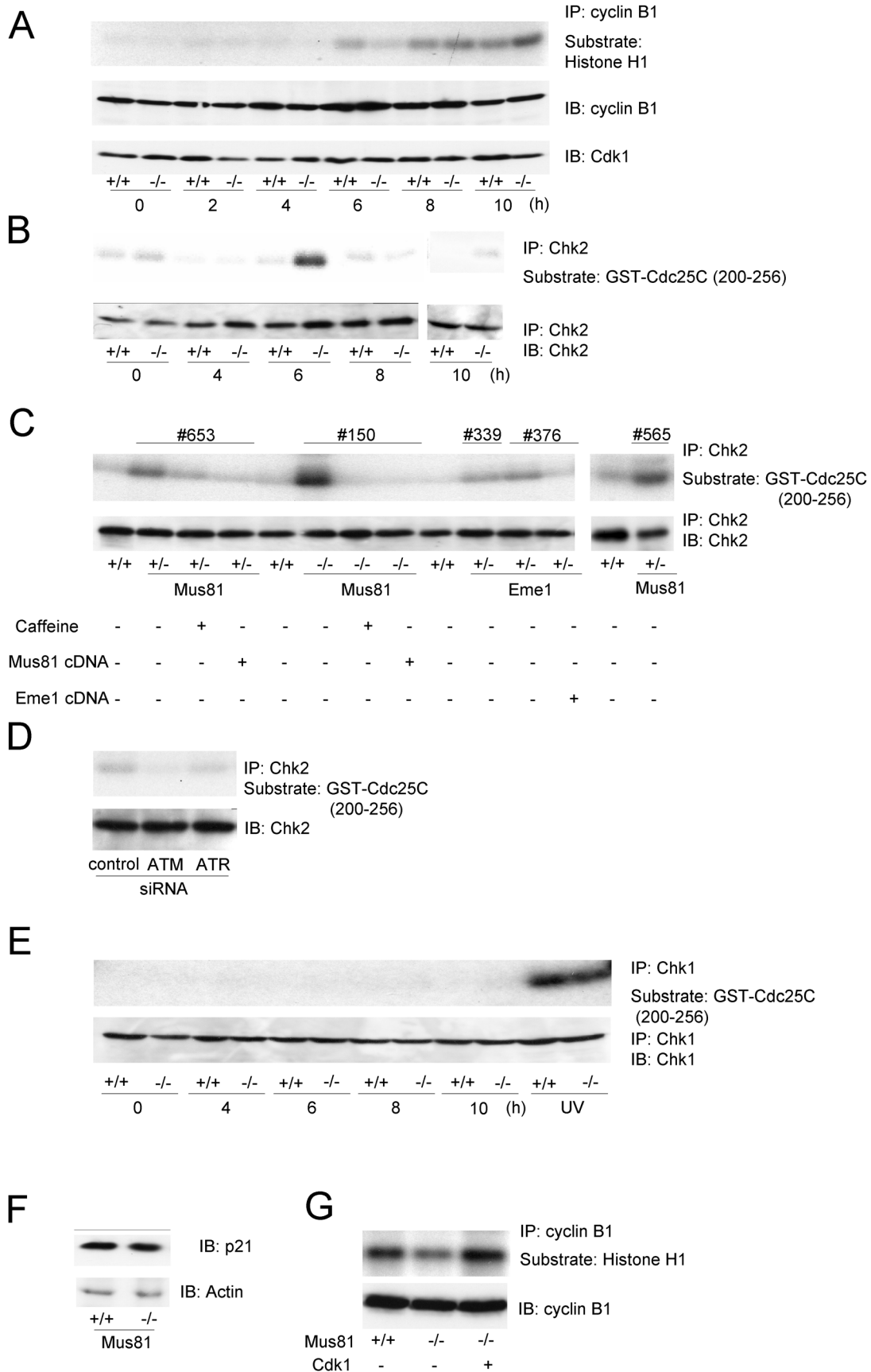
Overexpression of Cdk1 prevents rereplication

Because deletion of Cdk1 promotes DNA rereplication in human cells (42), reduced cyclin B kinase activity is likely to cause increased rereplication in Mus81 mutants. We examined this possibility by overexpressing Cdk1 in the Mus81 mutants. Cdk1 kinase activity is regulated by accumulation of Cdk1-associated cyclin B and removal of inhibitory protein phosphorylations. Western blot analysis revealed that levels of cyclin B were high in G$_2$/M in *Mus81*$^{-/-}$ cells while the levels of Cdk1 were constant, suggesting that overexpressed Cdk1 may be associated with endogenous cyclin B. Given that overexpressed Cdk1 is not phosphorylated on inhibitory phosphorylation sites by overcoming Wee1 and Myt1 kinase activities, Cdk1 activity is expected to be increased. Because we showed that p21 is not induced in *Mus81*$^{-/-}$, it is not necessary to consider direct inhibition of Cdk2 activity by p21. Consistent with this hypothesis, the reduction of cyclin B kinase activity was reversed by the overexpression of Cdk1 (Figure 6G). The increase in cyclin B activity by ectopic expression of Cdk1 reduced the frequency of tetraploidy from 2.46 to 0.50% and 0.54% in the two *Mus81*$^{-/-}$ cell lines ($P < 1.0 \times 10^{-2}$) (Table 1). Thus, the increased rereplication in Mus81 mutants was reversed by ectopic expression of Cdk1.

DISCUSSION

In the current studies, we demonstrated that Mus81–Eme1 deficiency activates the intra-S-phase and G$_2$/M checkpoints in response to DNA damage and promotes DNA rereplication. In addition, we confirmed that the Mus81–Eme1 complex contributes to the resistance against DNA-damaging agents in human cells. These assays show quite small differences, suggesting that there may be functional redundancy between the Mus81–Eme1 complex and other repair proteins in the response to DNA damage. Consistent with extensive genetic studies in yeast, the results of the present study indicate that there is no functional difference between Mus81 and Eme1 in human cells.

Identification of the physiological substrates of the Mus81–Eme1 complex has long remained elusive. However, a study showing the presence of resolvase activities in two separate fractions from human cell extracts has significantly enhanced our understanding of this complex system (43,44). The Mus81–Eme1 complex shows a greater activity for the

A

IP: cyclin B1

Substrate:
Histone H1

IB: cyclin B1

IB: Cdk1

| +/+ | -/- | +/+ | -/- | +/+ | -/- | +/+ | -/- | +/+ | -/- | +/+ | -/- | |
| 0 | | 2 | | 4 | | 6 | | 8 | | 10 | | (h) |

B

IP: Chk2

Substrate: GST-Cdc25C (200-256)

IP: Chk2
IB: Chk2

| +/+ | -/- | +/+ | -/- | +/+ | -/- | +/+ | -/- | +/+ | -/- | |
| 0 | | 4 | | 6 | | 8 | | 10 | | (h) |

C

#653   #150   #339 #376   #565

IP: Chk2

Substrate: GST-Cdc25C
(200-256)

IP: Chk2
IB: Chk2

| +/+ | +/- | +/- | +/- | +/+ | -/- | -/- | -/- | +/+ | +/- | +/- | +/- | +/+ | +/- |
| | Mus81 | | | | Mus81 | | | | Eme1 | | | | Mus81 |

Caffeine	-	-	+	-	-	-	+	-	-	-	-	-	-	-
Mus81 cDNA	-	-	-	+	-	-	-	+	-	-	-	-	-	-
Eme1 cDNA	-	-	-	-	-	-	-	-	-	-	-	+	-	-

D

IP: Chk2
Substrate: GST-Cdc25C
(200-256)

IB: Chk2

control ATM ATR
siRNA

E

IP: Chk1

Substrate: GST-Cdc25C
(200-256)

IP: Chk1
IB: Chk1

| +/+ | -/- | +/+ | -/- | +/+ | -/- | +/+ | -/- | +/+ | -/- | +/+ | -/- |
| 0 | | 4 | | 6 | | 8 | | 10 | (h) | UV | |

F

IB: p21

IB: Actin

+/+   -/-
Mus81

G

IP: cyclin B1
Substrate: Histone H1

IB: cyclin B1

| Mus81 | +/+ | -/- | -/- |
| Cdk1 | - | - | + |

3′-flap and three-way branched fork structures, whereas the Rad51C complex shows specific activity for Holliday junctions. These findings suggest that replication forks or 3′-flaps may be the *in vivo* substrates of the Mus81 endonuclease. The present finding that the Mus81–Eme1 complex confers resistance to DNA crosslinking agents, MMS and hydroxyurea supports this idea because these agents cause stalled replication forks. However, it is also possible that recombination intermediates such as D-loops and Holliday junctions are the *in vivo* substrates of the endonuclease. This possibility is supported by the observation that mutations in genes such as *RAD51*, *RAD52*, *RAD55* and *RAD57* that play early roles in recombination suppress the synthetic lethality of *mus81* (or *mms4*) *sgs1* (or *top3*) mutants (45,46). If Mus81-Mms4 directly cleaves replication forks and does not play a late role, synthetic lethality would not be rescued by a defect in these genes. The physical interaction of Mus81 with Rad54 in yeast is consistent with this idea (5). Furthermore, Mus81 has been shown to play a key role in the Rhp51-independent recombination repair pathway in fission yeast by resolving D-loops formed by Rad22 (47).

We observed spontaneous activation of the intra-S-phase checkpoint through two independent cascades in $Mus81^{-/-}$ cells. The ATM-Chk2-Cdc25A-Cdk2 pathway has been shown to play a role in the intra-S-phase checkpoint in response to DSBs. In addition, the damage-dependent Chk1 pathway was activated by ATM but not by ATR. This finding strongly suggests that the Mus81–Eme1 complex is involved in the processing of DSBs. This notion is also supported by the present finding that Mus81 or Eme1 deficiency led to the activation of the G_2/M checkpoint through the ATM-Chk2 pathway. DSBs that escape the intra-S-phase checkpoint and/or DSBs generated in G_2 can activate the G_2/M checkpoint. Thus, the recombination intermediates are likely to be the *in vivo* target of the Mus81–Eme1 complex. It is also possible that stalled replication forks, if unprocessed, generate DSBs, which could activate the ATM-dependent checkpoint pathway. In contrast to ATM, ATR kinase activity is activated by several kinds of DNA damage, including those caused by UV radiation and chemicals that make bulky base lesions, as well as by stalled replication forks (48). Although the present study demonstrated that Chk1 is not activated by ATR, it is very likely that ATR was activated in $Mus81^{-/-}$ cells. Despite the fact that cyclin A activity was strongly repressed, activation of Chk1 and Chk2 could account for the S phase delay only in a small proportion of the Mus81 and Eme1 mutant cells. In addition to the intra-S-phase checkpoint, the replication checkpoint initiated by ATR is likely to play a major role in the S phase delay resulting from Mus81 or Eme1 deficiency. Identification of the effectors that protect the replication fork will address this issue.

Mus81 has been shown to be physically associated with Cds1 (Chk2) in yeast and in human cells, suggesting a functional link between these proteins. We found that ionizing radiation- or MMC-induced phosphorylation of Chk2 on Thr-68 is not affected by a deficiency of Mus81 (data not shown), suggesting that Mus81 does not directly regulate the function of Chk2. Conversely, phosphorylation of Mus81 by Chk2 has been shown to be required for the maintenance of genome integrity during replication stress (19).

Evidence for the molecular mechanisms underlying checkpoint activation in response to DNA damage has largely come from studies in cells exposed to DNA-damaging agents. In contrast to these studies, our results provide new insight into the mechanism of checkpoint activation in response to DNA damage that spontaneously arises from a defect in a single process of DNA repair where there is no exogenous DNA damage. Reactive cellular metabolites are assumed to become endogenous genotoxic insults. Because the cells were more sensitive to DNA crosslinking agents than other agents, it is of interest to identify the sources of endogenous DNA interstrand crosslinks.

In addition to increased chromosomal aberrations such as gaps and breaks, we found increased frequencies of tetraploidy in the Mus81–Eme1 mutants. In yeast, B-type cyclin-dependent kinases prevent rereplication by several overlapping mechanisms, including phosphorylation of ORC, down-regulation of Cdc6 and nuclear exclusion of MCM proteins (49). The ability of these kinases to prevent rereplication is also supported by the finding that cyclin B/Cdk1 is associated with replication origins (50). In human cells, deletion of Cdk1 by gene targeting results in increased levels of tetraploidy (42). It is therefore likely that reduced cyclin B/Cdk1 kinase activity caused increased rereplication in the Mus81 mutants. This model is supported by our finding that the overexpression of Cdk1 prevents rereplication in Mus81 mutants, although we cannot exclude the possibility that Cdk1 overexpression plays an indirect role in preventing rereplication. Chromosomes in tetraploid cells are very unstable, as demonstrated by the finding that tetraploid-derived mouse tumors have numerical and structural chromosomal aberrations (51). The aneuploidy observed in mouse $Mus81^{-/-}$ cells may result from chromosome instability in tetraploid cells. Recent evidence has suggested that aneuploid cells proceed through a tetraploid state (52). This possibility may also account for the absence of a clear peak of 8C DNA content in $Mus81^{-/-}$ cells in FACS profiles. We observed extremely low frequency of DNA contents ranging from 4C to 8C at high magnification, which apparently concealed a small peak at 8C.

Haploinsufficiency of *Mus81* was found to cause phenotypes similar to those of a complete loss of the gene. Similar results were observed for $Mus81^{+/-}$ and $Mus81^{-/-}$ mice. Loss

Figure 6. Activation of the G_2/M checkpoint. (**A**) Cyclin B kinase activity with histone H1 as the substrate. Wild-type and $Mus81^{-/-}$ (#150) cells were synchronized in G_1/S by double-thymidine block and released. (**B**) Chk2 kinase activity using GST-Cdc25C (200–256) as the substrate and whole-cell extracts from wild-type and $Mus81^{-/-}$ (#150) cells synchronized in G_1/S and released. The experiments in (A) and (B) were performed five times. (**C**) Chk2 kinase activity on GST-Cdc25C (200–256) of synchronized cells harvested 6 h after release. For caffeine treatment, cells were incubated in the presence of 0.5 mM caffeine for 1 h prior to cell lysis. (**D**) The effects of ATM and ATR on Chk2 activity. Shown is the Chk2 kinase activity using GST-Cdc25C (200–256) as a substrate in extracts of $Mus81^{-/-}$ (#150) cells harvested 48 h after transfection with siRNA. (**E**) Chk1 kinase activity using GST-Cdc25C (200–256) as a substrate in extracts from wild-type and $Mus81^{-/-}$ (#150) cells synchronized in G_1/S and released. Cells treated with UV radiation are used as positive controls. The treated cells were harvested 5 h after UV radiation (40 J/m²). The experiments in (C), (D) and (E) were performed twice, and representative results are shown. (**F**) Western blot analysis of extracts from unsynchronized cells using an anti-p21 antibody. (**G**) Cyclin B kinase activity with histone H1 as a substrate in extracts from unsynchronized cells. In (F) and (G), $Mus81^{-/-}$ (#150) cells were used.

of heterozygosity is commonly observed in tumors. The human *Mus81* gene maps to chromosome 11q13.1. Although loss of heterozygosity at the *Mus81* locus in tumors has not been reported, normal or precancerous cells have a chance to lose one allele of *Mus81*. Given that cells lose one copy of *Mus81* during tumor progression, aberrant replication fork structures and recombination intermediates are expected to accumulate and eventually lead to further genomic instability. Haploinsufficiency of *Mus81* may contribute to tumor progression through this mechanism. It is noteworthy that predisposition to cancer was not observed over 15 months in another *Mus81*$^{-/-}$ mouse model (7). This discrepancy may be explained by a difference in strains. However, it is most likely that Mus81 deficiency does not directly contribute to tumor formation but rather induces chromosome aberrations such as aneuploidy that do not directly lead to cancer. A long latency, during which chromosomal aberrations accumulate, may be required for tumor formation in such a situation. It is also possible that additional modifiers that promote different types of genomic instability are required for tumor formation.

The present finding that small changes in the gene dosage of Mus81–Eme1 promote rereplication implicates the significance of small amounts of genotoxic insults in chromosome stability. Even in the absence of exogenous genotoxic sources, endogenous insults can lead to chromosome instability by damaging DNA. Aberrant fork structures and recombination intermediates are expected to accumulate in cells exposed to genotoxic insults. These cells suffer from increased rereplication in response to DNA damage, which does not immediately lead to tumor-associated genomic aberrations. Instead, this pathway can contribute to tumor development by inducing centrosome dysfunction and aneuploidy after numerous rounds of the cell cycle. This scenario may explain cases of radiation-induced carcinogenesis in which patients develop tumors after long periods of exposure to low-dose radiation.

ACKNOWLEDGEMENTS

REFERENCES

1. Branzei,D. and Foiani,M. (2005) The DNA damage response during DNA replication. *Curr. Opin. Cell Biol.*, **17**, 568–575.
2. Sancar,A., Lindsey-Boltz,L.A., Unsal-Kacmaz,K. and Linn,S. (2004) Molecular mechanisms of mammalian DNA repair and the DNA damage checkpoints. *Annu. Rev. Biochem.*, **73**, 39–85.
3. Lambert,S., Watson,A., Sheedy,D.M., Martin,B. and Carr,A.M. (2005) Gross chromosomal rearrangements and elevated recombination at an inducible site-specific replication fork barrier. *Cell*, **121**, 689–702.
4. Boddy,M.N., Lopez-Girona,A., Shanahan,P., Interthal,H., Heyer,W.-D. and Russell,P. (2000) Damage tolerance protein Mus81 associates with the FHA1 domain of checkpoint kinase Cds1. *Mol. Cell. Biol.*, **20**, 8758–8766.
5. Interthal,H. and Heyer,H.-D. (2000) *MUS81* encodes a novel Helix-hairpin-Helix protein involved in the response to UV- and methylation-induced DNA damage in *Saccharomyces cerevisiae*. *Mol. Gen. Genet.*, **263**, 812–827.
6. Doe,C.L., Ahn,J.S., Dixon,J. and Whitby,M.C. (2002) Mus81-Eme1 and Rqh1 involvement in processing stalled and collapsed replication forks. *J. Biol. Chem.*, **277**, 32753–32759.
7. Dendouga,N., Gao,H., Moechars,D., Janicot,M., Vialard,J. and McGowan,C.H. (2005) Disruption of murine Mus81 increases genomic instability and DNA damage sensitivity but does not promote tumorigenesis. *Mol. Cell. Biol.*, **25**, 7569–7579.
8. Kaliraman,V., Mullen,J.R., Fricke,W.M., Bastin-Shanower,S.A. and Brill,S.J. (2001) Functional overlap between Sgs1-Top3 and the Mms4-Mus81 endonuclease. *Genes Dev.*, **15**, 2730–2740.
9. Boddy,M.N., Gaillard,P.-H.L., McDonald,W.H., Shanahan,P., Yates,J.R.,III and Russell,P. (2001) Mus81-Eme1 are essential components of a Holliday junction resolvase. *Cell*, **107**, 537–548.
10. Abraham,J., Lemmers,B., Hande,M.P., Moynahan,M.E., Chahwan,C., Ciccia,A., Essers,J., Hanada,K., Chahwan,R., Khaw,A.K. *et al.* (2003) Eme1 is involved in DNA damage processing and maintenance of genomic stability in mammalian cells. *EMBO J.*, **22**, 6137–6147.
11. Blais,V., Gao,H., Elwell,C.A., Boddy,M.N., Gaillard,P.-H.L., Russell,P. and McGowan,C.H. (2004) RNA interference inhibition of Mus81 reduces mitotic recombination in human cells. *Mol. Biol. Cell*, **15**, 552–562.
12. Ciccia,A., Constantinou,A. and West,S.C. (2003) Identification and characterization of the human Mus81-Eme1 endonuclease. *J. Biol. Chem.*, **278**, 25172–25178.
13. Ogrunc,M. and Sancar,A. (2003) Identification and characterization of human MUS81-MMS4 structure specific endonuclease. *J. Biol. Chem.*, **278**, 21715–21720.
14. Chen,X.-B., Melchionna,R., Denis,C.-M., Gaillard,P.-H.L., Blasina,A., Van de Weyer,I., Boddy,M.N., Russell,P., Vialard,J. and McGowan,C.H. (2001) Human Mus81-associated endonuclease cleaves Holliday junctions *in vitro*. *Mol. Cell*, **8**, 1117–1127.
15. Gaillard,P.-H.L., Noguchi,E., Shanahan,P. and Russell,P. (2003) The endogenous Mus81–Eme1 complex resolves Holliday junctions by a nick and counternick mechanism. *Mol. Cell*, **12**, 747–759.
16. Osman,F., Dixon,J., Doe,C.L. and Whitby,M.C. (2003) Generating crossovers by resolution of nicked Holliday junctions: a role for Mus81-Eme1 in meiosis. *Mol. Cell*, **12**, 761–774.
17. de los Santos,T., Loidl,J., Larkin,B. and Hollingsworth,N.M. (2001) A role for *MMS4* in the processing of recombination intermediates during meiosis in *Saccharomyces cerevisiae*. *Genetics*, **159**, 1511–1525.
18. McPherson,J.P., Lemmers,B., Chahwan,R., Pamidi,A., Migon,E., Matysiak-Zablock,E., Moynahan,M.E., Essers,J., Hanada,K., Poonepalli,A. *et al.* (2004) Involvement of mammalian Mus81 in genome integrity and tumor suppression. *Science*, **304**, 1822–1826.
19. Kai,M., Boddy,M.N., Russell,P. and Wang,T.S.-F. (2005) Replication checkpoint kinase Cds1 regulates Mus81 to preserve genome integrity during replication stress. *Genes Dev.*, **19**, 919–932.
20. Michel,L.S., Liberal,V., Chatterjee,A., Kirchwegger,R., Pasche,B., Gerald,W., Dobles,M., Sorger,P.K., Murty,V.V. and Benezra,R. (2001) MAD2 haplo-insufficiency causes premature anaphase and chromosome instability in mammalian cells. *Nature*, **409**, 355–359.
21. Miyagawa,K., Tsuruga,T., Kinomura,A., Usui,K., Katsura,M., Tashiro,S., Mishima,H. and Tanaka,K. (2002) A role for *RAD54B* in homologous recombination in human cells. *EMBO J.*, **21**, 175–180.
22. Yoshihara,T., Ishida,M., Kinomura,A., Katsura,M., Tsuruga,T., Tashiro,S., Asahara,T. and Miyagawa,K. (2004) XRCC3 deficiency results in a defect in recombination and increased endoreduplication in human cells. *EMBO J.*, **23**, 670–680.
23. Wassmann,K. and Benezra,R. (1998) Mad2 transiently associates with an APC/p55Cdc complex during mitosis. *Proc. Natl Acad. Sci. USA*, **95**, 11193–11198.
24. Gao,H., Chen,X.-B. and McGowan,C.H. (2003) Mus81 endonuclease localizes to nucleoli and to regions of DNA damage in human S phase cells. *Mol. Biol. Cell*, **14**, 4826–4834.
25. Tashiro,S., Walter,J., Shinohara,A., Kamada,N. and Cremer,T. (2000) Rad51 accumulation at sites of DNA damage and in postreplicative chromatin. *J. Cell. Biol.*, **150**, 283–291.

26. Bishop,D.K., Ear,U., Bhattacharyya,A., Calderone,C., Beckett,M., Weichselbaum,R.R. and Shinohara,A. (1998) Xrcc3 is required for assembly of Rad51 complexes *in vivo*. *J. Biol. Chem.*, **273**, 21482–21488.
27. Takata,M., Sasaki,M.S., Tachiiri,S., Fukushima,T., Sonoda,E., Schild,D., Thompson,L.H. and Takeda,S. (2001) Chromosome instability and defective recombinational repair in knockout mutants of the five Rad51 paralogs. *Mol. Cell. Biol.*, **21**, 2858–2866.
28. Solinger,J.A., Kiianitsa,K. and Heyer,W.-D. (2002) Rad54, a Swi2/Snf2-like recombinational repair protein, disassembles Rad51:dsDNA filaments. *Mol. Cell*, **10**, 1175–1188.
29. Tan,T.L.R., Essers,J., Citterio,E., Swagemakers,S.M.A., de Wit,J., Benson,F.E., Hoeijmakers,J.H.J. and Kanaar,R. (1999) Mouse Rad54 affects DNA conformation and DNA-damage-induced Rad51 foci formation. *Curr. Biol.*, **9**, 325–328.
30. Thompson,L.H. and Schild,D. (2001) Homologous recombinational repair of DNA ensures mammalian chromosome stability. *Mutat. Res.*, **477**, 131–153.
31. Bartek,J., Lukas,C. and Lukas,J. (2004) Checking on DNA damage in S phase. *Nature Rev. Mol. Cell Biol.*, **5**, 792–804.
32. Sorensen,C.S., Syljuasen,R.G., Falck,J., Schroeder,T., Ronnstrand,L., Khanna,K.K., Zhou,B.-B., Bartek,J. and Lukas,J. (2003) Chk1 regulates the S phase checkpoint by coupling the physiological turnover and ionizing radiation-induced accelerated proteolysis of Cdc25A. *Cancer Cell*, **3**, 247–258.
33. Falck,J., Mailand,N., Syljuasen,R.G., Bartek,J. and Lukas,J. (2001) The ATM-Chk2-Cdc25A checkpoint pathway guards against radioresistant DNA synthesis. *Nature*, **410**, 842–847.
34. Shen,M., Feng,Y., Gao,C., Tao,D., Hu,J., Reed,E., Li,Q.Q. and Gong,J. (2004) Detection of cyclin B1 expression in G_1 phase cancer cell lines and cancer tissues by postsorting western blot analysis. *Cancer Res.*, **64**, 1607–1610.
35. Iliakis,G., Wang,Y., Guan,J. and Wang,H. (2003) DNA damage checkpoint control in cells exposed to ionizing radiation. *Oncogene*, **22**, 5834–5847.
36. Matsuoka,S., Huang,M. and Elledge,S.J. (1998) Linkage of ATM to cell cycle regulation by the Chk2 protein kinase. *Science*, **282**, 1893–1897.
37. Kaufmann,W.K., Heffernan,T.P., Beaulieu,L.M., Doherty,S., Frank,A.R., Zhou,Y., Bryant,M.F., Zhou,T., Luche,D.D., Nikolaishvili-Feinberg,N. *et al.* (2003) Caffeine and human DNA metabolism: the magic and the mystery. *Mutat. Res.*, **532**, 85–102.
38. Blasina,A., Price,B.D., Turenne,G.A. and McGowan,C.H. (1999) Caffeine inhibits the checkpoint kinase ATM. *Curr. Biol.*, **9**, 1135–1138.
39. Sarkaria,J.N., Busby,E.C., Tibbetts,R.S., Roos,P., Taya,Y., Karnitz,L.M. and Abraham,R.T. (1999) Inhibition of ATM and ATR kinase activities by the radiosensitizing agent, caffeine. *Cancer Res.*, **59**, 4375–4382.
40. Zhou,B.-B.S., Chaturvedi,P., Spring,K., Scott,S.P., Johanson,R.A., Mishra,R., Mattern,M.R., Winkler,J.D. and Khanna,K.K. (2000) Caffeine abolishes the mammalian G_2/M DNA damage checkpoint by inhibiting ataxia-telangiectasia-mutated kinase activity. *J. Biol. Chem.*, **275**, 10342–10348.
41. Lukas,J., Lukas,C. and Bartek,J. (2004) Mammalian cell cycle checkpoints: signaling pathways and their organization in space and time. *DNA Repair*, **3**, 997–1007.
42. Itzhaki,J.E., Gilbert,C.S. and Porter,A.C.G. (1997) Construction by gene targeting in human cells of a 'conditional' *CDC2* mutant that rereplicates its DNA. *Nature Genet.*, **15**, 258–265.
43. Constantinou,A., Chen,X.-B., McGowan,C.H. and West,S.C. (2002) Holliday junction resolution in human cells: two junction endonucleases with distinct substrate specificities. *EMBO J.*, **21**, 5577–5585.
44. Liu,Y., Masson,J.-Y., Shah,R., O'Regan,P. and West,S.C. (2004) RAD51C is required for Holliday junction processing in mammalian cells. *Science*, **303**, 243–246.
45. Bastin-Shanower,S.A., Fricke,W.M., Mullen,J.R. and Brill,S.J. (2003) The mechanism of Mus81-Mms4 cleavage site selection distinguishes it from the homologous endonuclease Rad1-Rad10. *Mol. Cell. Biol.*, **23**, 3487–3496.
46. Fabre,F., Chan,A., Heyer,W.-D. and Gangloff,S. (2002) Alternate pathways involving Sgs1/Top3, Mus81/Mms4, and Srs2 prevent formation of toxic recombination intermediates from single-stranded gaps created by DNA replication. *Proc. Natl Acad. Sci. USA*, **99**, 16887–16892.
47. Doe,C.L., Osman,F., Dixon,J. and Whitby,M.C. (2004) DNA repair by a Rad22-Mus81-dependent pathway that is independent of Rhp51. *Nucleic Acids Res.*, **32**, 5570–5581.
48. Abraham,R.T. (2001) Cell cycle checkpoint signaling through the ATM and ATR kinases. *Genes Dev.*, **15**, 2177–2196.
49. Nguyen,V.Q., Co,C. and Li,J.J. (2001) Cyclin-dependent kinases prevent DNA re-replication through multiple mechanisms. *Nature*, **411**, 1068–1073.
50. Wuarin,J., Buck,V., Nurse,P. and Millar,J.B.A. (2002) Stable association of mitotic Cyclin B/Cdc2 to replication origins prevents endoreduplication. *Cell*, **111**, 419–431.
51. Fujiwara,T., Bandi,M., Nitta,M., Ivanova,E.V., Bronson,R.T. and Pellman,D. (2005) Cytokinesis failure generating tetraploids promotes tumorigenesis in *p53*-null cells. *Nature*, **437**, 1043–1047.
52. Shi,Q. and King,R.W. (2005) Chromosome nondisjunction yields tetraploid rather than aneuploid cells in human cell lines. *Nature*, **437**, 1038–1042.